

Final Report

Study of Nonlinear Interaction and Turbulence of Alfvén Waves in LAPD Experiments

DE-SC0001794

Covered period: 8/15/09 - 8/15/13

PI: Stanislav Boldyrev, Co-PI: Jean Carlos Perez

Department of Physics, 1150 University Ave, University of Wisconsin, Madison, Wisconsin 53806; Email: boldyrev@wisc.edu; telephone: (608)262-2338

November 29, 2013

Magnetic turbulence is ubiquitous in astrophysical systems and it is present in laboratory devices. Turbulence may be naturally generated due to various instabilities (such as supernovae explosions and galactic shear in the interstellar medium, magnetorotational instability in accretion disks, tearing modes in Madison Symmetric Torus (MST) experiment, shear flows in Large Plasma Device (LAPD) experiments, etc). Nonlinear energy cascade transfers the energy to smaller and smaller scales, thus distributing turbulent energy over a broad range of scales.

It has become evident from analytic and numerical results that the character of magnetic turbulence crucially depends on how counterpropagating Alfvén wave packets interact with each other. A laboratory study of nonlinearly interacting Alfvén waves is helpful in this respect, since it provides an opportunity for studying such individual interactions. The same processes can be effectively modeled numerically, and detailed comparison can be made with laboratory data. The complete project had two major goals — investigate MHD turbulence generated by counterpropagating Alfvén modes, and study such processes in the LAPD device.

In order to study MHD turbulence in numerical simulations, two codes have been used: full MHD, and reduced MHD developed specially for this project.

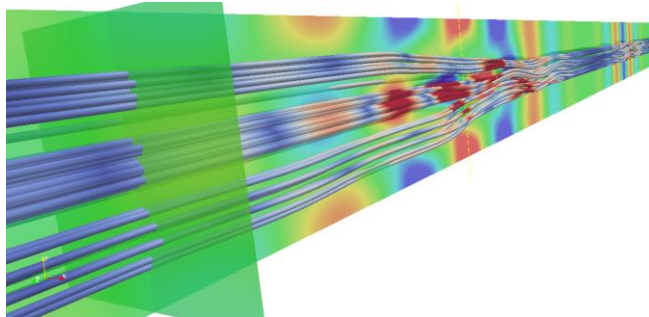


FIG. 1: Magnetic field lines during a collision of two counterpropagating Alfvén wave packets. Vertical blue and orange lines (regions of vorticity) indicate the wave packet moving toward us, blue and orange spots indicate the wave packet moving from us. The interaction region is marked by the vertical white dashed line. Interaction leads to displacement and shuffling of magnetic field lines.

Quantitative numerical results are obtained through high-resolution simulations of strong MHD turbulence, performed through the 2010 DOE INCITE allocation; they are shown in Fig. 2. The simulations had the resolution up to 2048^3 collocation points, and statistics accumulated over 30

to 150 eddy turnover times. They constitute, to the best of our knowledge, the largest statistical sample of steady state magnetohydrodynamic turbulence available to date. We addressed the questions of the spectrum of turbulence, its universality, and the value of the so-called Kolmogorov constant (the normalization coefficient of the spectrum). The results are published in [Perez, Jean Carlos; Mason, Joanne; Boldyrev, Stanislav; Cattaneo, Fausto, *On the energy spectrum of strong magnetohydrodynamic turbulence*, Physical Review X (PRX) 2012, to appear.]

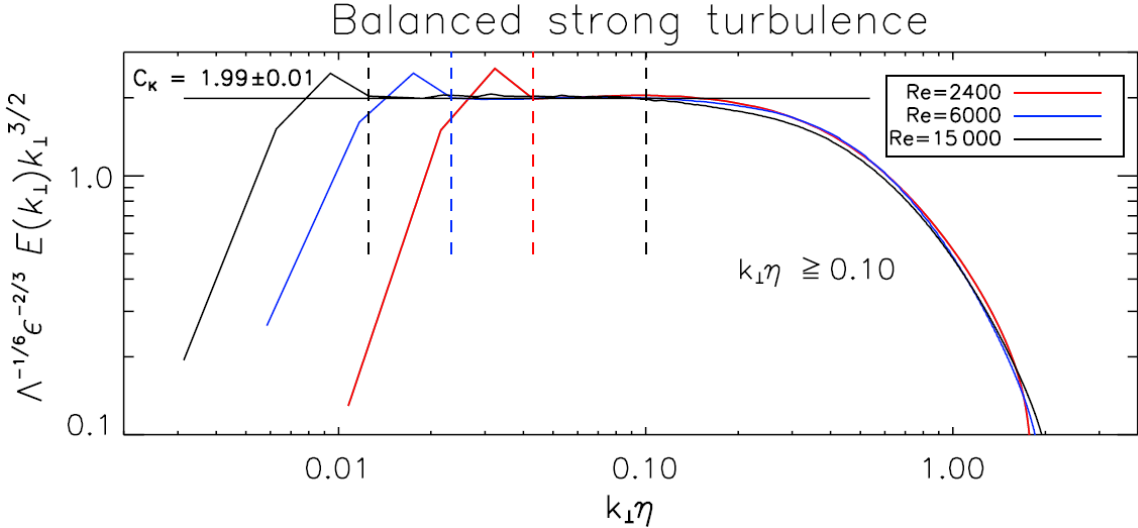


FIG. 2: Total field-perpendicular energy spectrum $E(k)$ in balanced strong MHD turbulence for different Reynolds numbers. The wave number is normalized by the dissipation scale η and the energy is compensated by $k_\perp^{3/2}$. The scale Λ is defined through the quantities of the inertial interval, as shown in [Perez et al PRX 2012]. The curves collapse onto each other (up to the forcing scale) revealing the universal functional form of the energy spectrum. These results confirm that the inertial-interval spectrum of strong incompressible MHD turbulence is close to $k^{-3/2}$. Besides, we established that the Kolmogorov constant can be defined in MHD turbulence, and its value is found to be $C \approx 2$.

In these simulations we measured with unprecedented accuracy the energy spectra of magnetic and velocity fluctuations. The total energy spectrum is shown in FIG. 2. We also studied the so-called residual energy, that is, the difference between kinetic and magnetic energies in turbulent fluctuations. Nonzero residual energy means that energy equipartition between the kinetic and magnetic modes is broken in the system. In our analytic work we explained generation of residual energy in weak MHD turbulence, in the process of random collisions of counter-propagating Alfvén waves. We then generalized these results for the case of strong MHD turbulence. The developed model explained generation of residual energy in strong MHD turbulence, and verified the results in numerical simulations. The analytic paper has been published in [Boldyrev, S.; Perez, J. C.; Wang, Y., ASP Conference Series, Vol. 459. (San

Francisco: Astronomical Society of the Pacific) 2012., p.3]. The numerical paper is currently in preparation.

We then analyzed the imbalanced case, where more Alfvén waves propagate in one direction. The solar wind is typically imbalanced, since more Alfvén waves propagate out of the sun. We found that spectral properties of the residual energy are similar for both balanced and imbalanced cases. In collaboration with Dr. Jean Perez (UW Madison), Drs. John Podesta and Joe Borovsky (Los alamos) we then compared strong MHD turbulence observed in the solar wind with turbulence generated in numerical simulations. The results are published in [S. Boldyrev, J.C. Perez, J. E. Borovsky, & J. J. Podesta ‘Spectral scaling laws in MHD turbulence simulations and in the solar wind’, submitted to *Astrophysical Journal Letters*. (2011).]

Nonlinear interaction of Alfvén waves has been studied in collaboration with Prof. Troy Carter’s group in the upgraded Large Plasma Device (LAPD) in UCLA. The LAPD device is 18 m long, ≤ 1 m diameter magnetized plasma column created by a pulsed discharge from a Barium Oxide coated emissive cathode. The typical plasma parameters in LAPD are $n_e \sim 5 \times 10^{22} \text{ cm}^{-3}$, $T_e \leq 15 \text{ eV}$, $T_i \leq 1 \text{ eV}$, $B < 0.2 \text{ T}$. In these experiments helium is used as a working gas. The plasma is created in pulsed discharges of $\sim 4 \text{ ms}$ every 1 s. The experimental set up is schematically shown in Fig. 3. Shear-Alfvén waves are generated by means of two antennas at both ends of the plasma column. Two magnetic probes are used on a shot-to-shot basis. One probe is fixed along the axis of the LAPD at the central point, while the other is placed 60 cm further along the main axis and can be moved in a rectangular grid of 41×40 positions perpendicular to the machine’s axis.

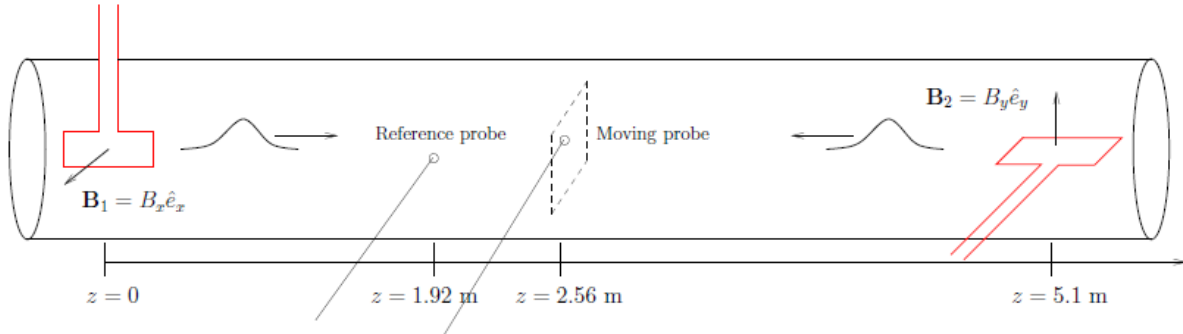


FIG 3: Experimental setup: two counter-propagating and colliding Alfvén waves are launched by the two antennae (red) on the opposite sides of the LAPD device

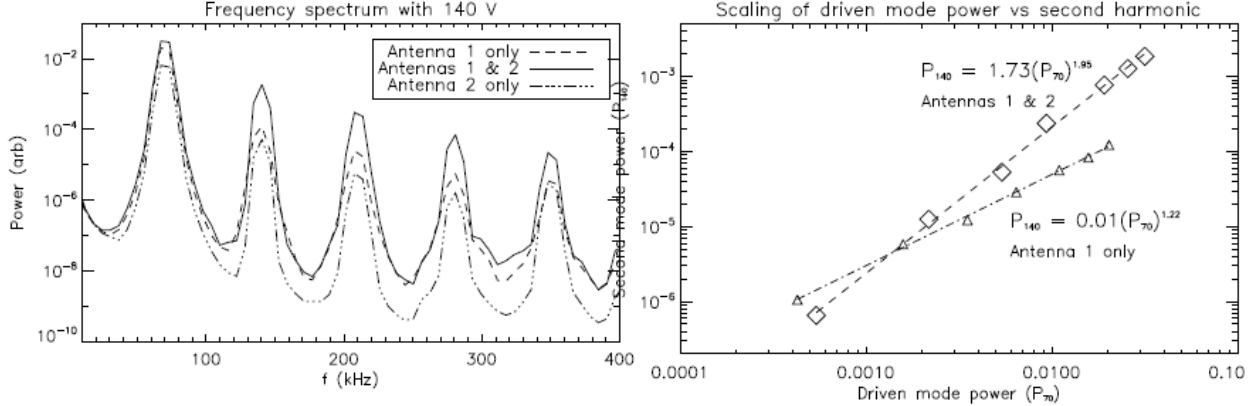


FIG 4: Wave packets generated by two independent antennae in LAPD experiments. The plot (left panel) shows the frequency spectra of the waves launched in the opposite directions (by antennae 1 & 2), and the spectrum of the resulting signal when both antennae are on. The plot in the right panel shows the intensity of the second harmonic as the function of the power in colliding waves. The almost quadratic scaling indicated the presence of nonlinear interactions.

We have simulated the collision of the Alfvén modes in the settings close to the experiment. We have created a train of wave packets with the amplitudes closed to those observed in the experiment, and allowed them to collide. We then saw the generation of the second harmonic, resembling that observed in the experiment (Fig. 5).

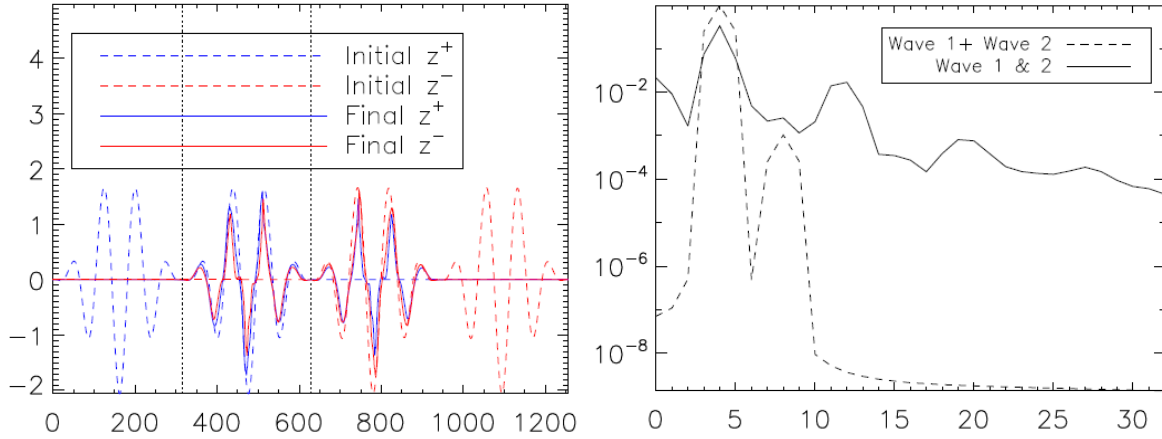


FIG 5: Left panel: wave patterns vs coordinate z (along the guide field) for a fixed point in the field-perpendicular plane. Dashed lines correspond to initial wave packets: two wave packets for each species z^{\pm} , with z^+ on one half of the box, and z^- on the other half. The solid lines are the wave patterns of z^{\pm} during first collision, i.e., when the leading wave packets completely overlap. The vertical dotted lines correspond to the region where the power spectrum is computed. Right panel: power spectrum of the waves during the collision. The dashed line corresponds to the linear superposition of the initial wave packets, and the solid line is the cross-field average power spectrum of the “signal” in the region of overlap (between vertical dotted lines in left panel).

The results of the project are presented in the following reviewed publications:

18. **Recent results on magnetic plasma turbulence,**
Boldyrev, S., Perez, J. C., Mason, J., Cattaneo, F., SOLAR WIND 13: Proceedings of the Thirteenth International Solar Wind Conference. [AIP Conf. Proceedings, Volume 1539, pp. 135-138 \(2013\)](#);
17. **Nature of Subproton Scale Turbulence in the Solar Wind,**
Chen, C. H. K., Boldyrev, S., Xia, Q., Perez, J. C., [Phys. Rev. Lett. 110 \(2013\) 225002, arXiv:1305.2950](#)
16. **Distribution of Magnetic Discontinuities in the Solar Wind and in MHD Turbulence,**
Zhdankin, V., Boldyrev, S., Mason, J., [Astrophys. J. Lett. 760 \(2012\) L22, arXiv:1210.3613](#)
15. **On the energy spectrum of strong magnetohydrodynamic turbulence,**
Perez, J. C., Mason, J., Boldyrev, S., Cattaneo, F., [Phys. Rev. X, 2 \(2012\) 041005, arXiv:1209.2011](#)
14. **Spectrum of kinetic-Alfvén turbulence,**
Boldyrev, S., Perez, J. C., [Astrophysical J. Lett., 758 \(2012\) L44, arXiv:1204.5809](#)
13. **Magnetic Discontinuities in Magnetohydrodynamic Turbulence and in the Solar Wind,**
Zhdankin, V., Boldyrev, S., Mason, J., Perez, J., [Phys. Rev. Lett. 108 \(2012\) 175004, arXiv:1204.4479](#)
12. **Residual Energy in Weak and Strong MHD Turbulence,**
Boldyrev, S., Perez, J. C., Wang, Y., ASP Conf. Series, Vol. 459. Edited by N.V. Pogorelov, J.A. Font, E. Audit, and G.P. Zank. 2012., p.3, [arXiv:1202.3453](#)
11. **Numerical simulations of strong incompressible magnetohydrodynamic turbulence,**
Mason, J., Perez, J. C., Boldyrev, S., Cattaneo, F., [Phys. Of Plasmas, 19 \(2012\) 055902 arXiv:1202.3474 \(2012\)](#)
10. **Residual Energy in Weak and Strong MHD Turbulence,**
Boldyrev, S., Perez, J. C., Wang, Y., In ASP Conference Series, 6th International Conference of Numerical Modeling of Space Plasma Flows (2011), Nikolai V. Pogorelov, Ed., [arXiv:1202.3453 \(2012\)](#)
9. **Spectral Scaling Laws in Magnetohydrodynamic Turbulence Simulations and in the Solar Wind,**
Boldyrev, S., Perez, J. C., Borovsky, J. E., Podesta, J. J., [Astrophys J. Lett 741, L19 \(2011\), arXiv:1106.0700 \(2011\)](#)
8. **Residual Energy in Magnetohydrodynamic Turbulence,**
Wang, Y. Boldyrev, S. Perez, J. C., [Astrophys. J. Lett., 740, L36 \(2011\) , arXiv:1106.2238 \(2011\)](#)
7. **Residual energy in in magnetohydrodynamic turbulence and in the solar wind,**
Boldyrev, S, Perez, J. C., Zhdankin, V., In "Physics of the Heliosphere: a 10-year Retrospective", Jacob Heerikhuisen, Gang Li, and Gary P. Zank, Eds., [arXiv:1108.6072 \(2011\)](#)
6. **Extended Scaling Laws in Numerical Simulations of Magnetohydrodynamic Turbulence,**
Mason, Joanne; Perez, Jean Carlos; Cattaneo, Fausto; Boldyrev, Stanislav, [Astrophys. J. Lett. 735, L26 \(2011\), arXiv:1104.1437](#)
5. **Magnetic Dynamo Action in Random Flows with Zero and Finite Correlation Times,**
Mason, J.; Malyshkin, L.; Boldyrev, S.; Cattaneo, F, [Astrophys. J. 730, 86 \(2011\).](#)
4. **MHD Dynamos and Turbulence,**
Tobias, Steven M.; Cattaneo, Fausto; Boldyrev, Stanislav.
A book chapter in 'Ten Chapters in Turbulence,' P. Davidson, Y. Kaneda, and K.R. Sreenivasan, eds., [arXiv:1103.3138 \(2013\).](#)
3. **Magnetic dynamo action at low magnetic Prandtl numbers,**

Malyshkin, L., Boldyrev, S. [Phys. Rev. Lett. 105, 215002 \(2010\)](#), arXiv:1011.0202 (2010)

2. **Strong magnetohydrodynamic turbulence with cross helicity,**
Perez, J.C., Boldyrev, S., [Phys. Plasmas 17, 055903 \(2010\)](#), arXiv:1004.3798 (2010).
1. **Numerical Simulations of Imbalanced Strong Magnetohydrodynamic Turbulence,**
Perez, J.C., Boldyrev, S., [Astrophys. J. 710, L63 \(2010\)](#); arXiv:0912.0901 (2010)